Frontiers and Results in Applied Sciences
https://www.iahiservices.com

Research Article

Aqueous Phase Reduction of Mn(VII) by Sulphide Ion: Kinetics, Thermodynamics and Stoichiometric Studies

Targema, Rosemary D[1]* Tivkaa Joseph T[2] Atagher, Comfort I[3]

[1,2] Department of Science Laboratory Technology, Benue State Polytechnic, P.M.B.01, Ugbokolo, Nigeria.
[3]Department of Food Science and Technology, Joseph Sarwuan Tarka University, Makurdi

*Corresponding Author Email: talktodooshis@gmail.com

Abstract- The reduction of Mn(VII) by sulphide ions (S^{2-}) in aqueous solution was investigated across pH 2–14, temperatures 303–323 K, and different reaction times. Concentration changes of Mn(VII) were monitored spectrophotometrically at 549 nm. Kinetic analysis confirmed a first-order dependence on Mn(VII), described by the rate law: Rate = $-d[MnO_4^-]/dt = -d[S^{2-}]/dt = k[MnO_4^-][S^{2-}]$. The reduction progressed with increasing time, temperature, and alkalinity. Higher rate constants (k_obs) were observed in alkaline media, attributed to OH^--induced formation of manganese oxyanions and hydroxo complexes that are more reactive toward S^{2-} than MnO_4^- itself. Thermodynamic parameters derived from ln(k_obs/T) versus 1/T plots revealed negative activation enthalpy ($\Delta H°$ = –7.32 to –43.40 kJ mol^{-1}), confirming the exothermic and spontaneous nature of the process. Positive activation entropy ($\Delta S°$ = 1.05–1.15 J K^{-1} mol^{-1}) indicated a dissociative mechanism with greater molecular randomness, while activation energies (9.91–45.96 kJ mol^{-1}) suggested relatively long transition-state bonds. Stoichiometric analysis showed a consistent Mn(VII):S^{2-} ratio of 0.23:1, independent of pH. Overall, the findings establish that sulphide ions effectively reduce Mn(VII) to more stable and less oxidizing lower oxidation states. The reaction generates intermediate manganese species and sulphate radicals, highlighting the Mn(VII)/S^{2-} system as a promising pathway for pollutant degradation and advanced water treatment applications.

Graphical Abstract

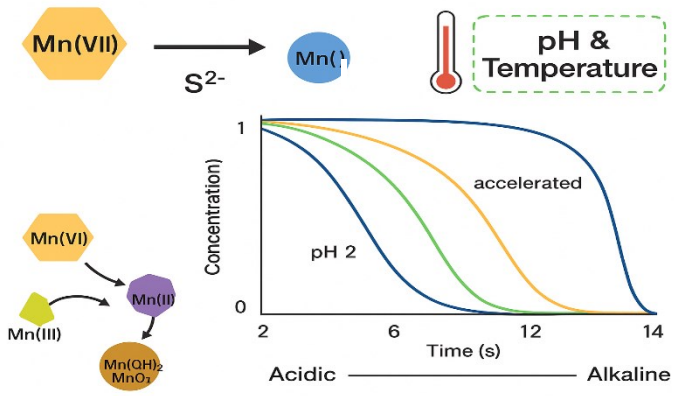

Article Key Information

Keywords: Sulphide ion, Mn(VII) reduction, Kinetics, Thermodynamics.

Received: 27th May 2025 **Revised:** 28th August 2025 **Accepted**: 19th September 2025 **Published**: 30th September 2025

1.0 Introduction

Manganese is a first-row transition metal belonging to Group 7 of the periodic table, along with technetium and rhenium. With atomic number 25 and atomic mass 54.94, manganese occurs naturally as the isotope ^{55}Mn and exhibits multiple oxidation states (+2, +3, +4, +6, +7), of which the +2 state is the most stable. It is the twelfth most abundant element in the Earth's crust, with an average upper crustal concentration of ~600 mg kg^{-1} and a bulk continental crust average of ~1400 mg kg^{-1} [1]. Among transition metals, only iron occurs at higher crustal concentrations. Manganese is widely distributed in nature, occurring in primary minerals such as pyrolusite (MnO_2), rhodochrosite ($MnCO_3$), and manganite (MnO(OH)), as well as within rock-forming silicates including garnet, olivine, pyroxene, amphibole, and calcite [2].

Biologically, manganese is an essential trace element required in small amounts for normal growth, skeletal development, metabolic regulation, and enzymatic redox functions [3]. At optimal concentrations, manganese contributes to neurological protection and glucose regulation. However, elevated exposure poses significant toxicological risks due to its bioaccumulative and non-biodegradable nature. Chronic overexposure has been linked to neurotoxicity, kidney dysfunction, DNA damage, and disorders of the central nervous system [4]–[6]. The dual role of manganese as both an essential micronutrient and a potential pollutant underscores its environmental and biomedical significance.

From an industrial perspective, permanganate (MnO_4^-, Mn(VII)) has emerged as a green and versatile oxidant. It is employed extensively for groundwater and soil remediation, oxidation of taste- and odor-causing compounds, and removal of Fe(II) and Mn(II) in water treatment [7]–[10]. Compared to other oxidants, permanganate is attractive for its stability, low cost, effectiveness over a broad pH range, and absence of chlorinated or brominated by-products. Its reduction products (Mn(III)/Mn(IV) solids) are environmentally benign and serve as useful coagulants and adsorbents in water treatment systems [11]. Nevertheless, the reactivity of Mn(VII) is highly structure-dependent, and its strong redox potential ($E° = +1.68$ V) does not guarantee universal effectiveness against diverse organic and inorganic pollutants. Moreover, manganese released during processing or disposal can persist in soils and aquatic environments, raising long-term ecological concerns [12].

Sulphide ions (S^{2-}) represent a promising reductant for Mn(VII) reduction due to their strong electron-donating capacity and the formation of sulphate as the primary, environmentally benign byproduct. The reduction of permanganate by sulphide not only lowers Mn(VII) to more stable oxidation states (primarily Mn^{2+}) but also promotes precipitation of $Mn(OH)_2$ or MnO_2 under alkaline conditions, facilitating removal by sedimentation or filtration. This makes sulphide particularly attractive for applications in wastewater treatment and metal detoxification [13].

The present study investigates the kinetics, thermodynamics, and stoichiometry of Mn(VII) reduction by sulphide ions in aqueous media. By elucidating reaction mechanisms across a wide pH and temperature range, this work provides fundamental insights into redox transformations of manganese while exploring the feasibility of sodium sulphide as an effective reductant for mitigating Mn(VII) toxicity in environmental systems.

2.0 Literature Review

The reduction of permanganate (Mn(VII)) by hydrogen peroxide (H_2O_2) has been extensively studied as a pathway for enhanced micropollutant abatement in water treatment systems. Xu and Von Gunten [14] reported that Mn(VII) reduction occurred within the pH range of 6.0–8.5 and exhibited a distinct lag phase followed by a rapid reduction to Mn(VI). The process was catalyzed by the deprotonated form of Mn(VI) through electron transfer within the [H_2O_2–$OMnO_3$] complex. At molar ratios of $[H_2O_2]_0$:$[Mn(VII)]_0 \leq 1$ and pH 7.5, a one-electron transfer mechanism predominated, yielding Mn(VI) and superoxide radicals (O_2^-) with near-quantitative radical yields relative to consumed Mn(VII). Importantly, the Mn(VII)–H_2O_2 system significantly enhanced the degradation of ciprofloxacin and its transformation products, demonstrating the potential for micropollutant control. The effect was suppressed when Mn(VII) was quenched by Ba^{2+}, underscoring the importance of Mn intermediates in the reaction pathway.

In the aqueous-phase reduction of Mn(VII) by sodium dithionite, Iorungwa et al. [15] observed that the reaction rate increased with temperature but decreased with pH. Thermodynamic analysis revealed negative activation entropy values (–104.89 to –113.66 J mol^{-1} K^{-1}), indicating a non-spontaneous, associative mechanistic pathway. Activation enthalpy values ranged widely (–8.68 × 10^2 to 4.78 × 10^3 kJ mol^{-1}), suggesting an overall endothermic process. The reduction was favored under acidic and neutral conditions, emphasizing the role of medium effects on reactivity.

Enhanced oxidation of organic contaminants using the Mn(VII)/bisulphite system has also been reported [16]. The efficiency of this process was influenced by the Mn(VII)/bisulphite molar ratio, solution pH, contaminant type, and water matrix composition. Rapid degradation occurred under acidic and neutral conditions, while alkaline conditions suppressed the process. Dissolved oxygen (DO) played a critical role by controlling the evolution of oxysulphur radicals and their subsequent interactions with reactive manganese species. Collectively, these findings highlight Mn(VII)/bisulphite as a promising strategy for wastewater treatment, particularly for acidic industrial effluents.

Beyond aqueous systems, redox transformations of sulphur species have been explored in geochemical contexts. Alonso-Azcarate et al. [17] investigated sulphur redox reactions and the formation of native sulphur veins during low-grade metamorphism of gypsum evaporites in the Cameros Basin (NE Spain). Using fluid inclusion homogenization and quartz–sulphate oxygen isotope geothermometry, they estimated vein formation temperatures of approximately 225 °C. The inclusions contained elemental sulphur (S^0) and gases such as H_2S, N_2, CO_2, and minor CH_4, consistent with thermochemical sulphate reduction (TSR) of organic matter followed by partial re-oxidation of H_2S by SO_4^{2-} to yield elemental sulphur.

At the biochemical level, Banerjee and Kabil [18] reviewed the redox biochemistry of hydrogen sulphide (H_2S). Disruption of γ-cystathionase in mice led to cardiovascular dysfunction and hypertension, demonstrating its critical role in vascular H_2S production. Interestingly, patients with inherited γ-cystathionase deficiency did not exhibit vascular pathologies, suggesting compensatory mechanisms. Furthermore, mitochondrial pathways for sulphide metabolism were shown to couple detoxification with oxidative phosphorylation, though at the risk of cytochrome c oxidase inhibition.

Electrochemical investigations have further advanced understanding of sulphur redox chemistry in energy systems. Lu et al. [19], using a rotating-ring disk electrode (RRDE), probed lithium–sulphur redox reactions in mixed organic electrolytes. They demonstrated that electrochemical steps of sulphur reduction were kinetically rapid but accounted for only ~25% of the theoretical capacity (≈4 e^-/S_8) within short timescales. Complete conversion to Li_2S required extended chemical polysulphide recombination and dissociation, occurring over hours in closed-cell batteries. These insights underscore the importance of both electrochemical and chemical steps in governing sulphur redox kinetics.

Taken together, these studies emphasize the diverse roles of permanganate and sulphur redox systems in environmental, geochemical, biological, and electrochemical contexts. The mechanistic variability across different reductants and environments underscores the importance of detailed kinetic and thermodynamic studies, such as the present investigation into Mn(VII) reduction by sulphide ions.

3.0 Materials and Methods

3.1 Apparatus and Reagents

The experimental work employed standard laboratory glassware and analytical instruments, including beakers, measuring cylinders, spatulas, volumetric flasks, Whatman No. 1 filter paper, and a stopwatch. Analytical-grade reagents (≥99% purity, Sigma Aldrich) were used without further purification: potassium permanganate ($KMnO_4$), sodium sulphide (Na_2S, source of S^{2-}), sulfuric acid (H_2SO_4), nitric acid (HNO_3), sodium hydroxide (NaOH), and biphenyl carbazide. The following instruments were utilized: a Unicom UV/Vis spectrophotometer, Oakton pH/Con 510 series pH meter, Adams PW 184 series electronic balance, thermostatic water bath, and a Manestay water distiller.

3.2 Preparation of Solutions

All solutions were prepared using distilled water. A 0.01 M Mn(VII) stock solution was prepared by dissolving 1.58 g of $KMnO_4$ (BDH) in 1 L of distilled water. Similarly, a 0.01 M sulphide stock solution was prepared by dissolving 1.0 g of Na_2S in 1 L of distilled water. To minimize interferences, two drops of biphenyl carbazide were added to the Mn(VII) solution before pH adjustment. Solution pH was adjusted using 1.0 M HCl for acidic conditions and 1.0 M NaOH for alkaline conditions, with precise measurements verified using a calibrated pH meter. Temperature control was achieved by immersing the $KMnO_4$ solution in a thermostatic water bath, with temperature verification provided by a thermometer.

3.3 Reduction of Mn(VII) by Sulphide Ion

The reduction of Mn(VII) by S^{2-} was carried out following the procedure outlined by Iorungwa et al. [20]. The UV/Vis spectrophotometer was set at 549 nm to monitor the absorbance of Mn(VII). For each experiment, 3 mL of the pH-adjusted, temperature-controlled Mn(VII) solution was transferred into a cuvette, to which 1 mL of sulphide solution was added. Absorbance was immediately recorded at 549 nm. All experiments were performed in triplicate, and the mean values were reported. Reactions were conducted at 303, 308, 313, 318, and 323 K.

To evaluate the effect of reaction time, separate mixtures were prepared and monitored at intervals of 0, 30, 60, 90, and 120 s, thereby avoiding disturbance from sample withdrawal. The experiments were performed at initial pH values of 2, 4, 6, 8, 10, 12, and 14.

Kinetic data were obtained by plotting the natural logarithm of Mn(VII) concentration versus time, from which the observed rate constant (k_{obs}) was derived as the slope. Thermodynamic parameters were obtained from plots of ln(k_obs/T) versus 1/T, using the Eyring equation:

$$\ln\left(\frac{k_{obs}}{T}\right) = \ln\left(\frac{k_b}{h}\right) + \frac{\Delta S^\circ}{R} - \frac{\Delta H^\circ}{RT} \qquad (1)$$

where T is absolute temperature (K), k_b is Boltzmann's constant (1.38×10^{-23} J/K), h is Planck's constant (6.63×10^{-34} J·s), and R is the universal gas constant (8.314 J K^{-1} mol^{-1}) [21].

The activation energy (E_a) was computed using the relationship:

$$E_a = \Delta H - T\Delta S \qquad (2)$$

[22]

Concentration dependence was evaluated using five reductant concentrations (4, 6, 8, 10, and 12 mg L^{-1}). These experiments were conducted at 298 K under moderately acidic (pH 5) and alkaline (pH 9) conditions. The initial Mn(VII) concentration was fixed at 10 mg L^{-1}, and reactions were monitored over 120 s using equal volumes (10 mL each) of Mn(VII) and sulphide solutions.

4.0 Results and Discussion

4.1 Kinetics of Mn(VII) Reduction by Sulphide Ion

The reduction of Mn(VII) by sulphide ion was monitored at varying temperatures (303–323 K) and pH conditions (2–14). The observed rate constants (k_obs) at different experimental conditions are presented in Table 1.

Table 1. Observed rate constants (kobs) for Mn(VII) reduction by S^{2-} at various pH and temperatures

pH	T (K)	kobs (s^{-1})	kobs/T ($s^{-1}\cdot K^{-1}$)	ln kobs	ln(kobs/T)	1/T (K^{-1})
2	303	1.10×10^{-2}	3.63×10^{-5}	–4.51	–10.22	0.00330
	308	1.15×10^{-2}	4.87×10^{-5}	–4.20	–9.93	0.00325
	313	1.19×10^{-2}	6.07×10^{-5}	–4.43	–9.71	0.00320
	318	2.10×10^{-2}	6.60×10^{-5}	–3.86	–9.63	0.00315
	323	2.30×10^{-2}	7.74×10^{-5}	–3.77	–9.47	0.00310
4	303	2.00×10^{-3}	6.60×10^{-6}	–6.22	–11.93	0.00330
	308	4.00×10^{-3}	1.30×10^{-5}	–5.52	–11.25	0.00325
	313	5.00×10^{-3}	1.60×10^{-5}	–5.29	–11.05	0.00320
	318	6.00×10^{-3}	1.88×10^{-5}	–5.12	–10.88	0.00315
	323	6.50×10^{-3}	2.01×10^{-5}	–5.04	–10.81	0.00310
6	303	2.00×10^{-2}	6.60×10^{-5}	–3.91	–9.63	0.00330
	308	2.50×10^{-2}	8.12×10^{-5}	–3.69	–9.42	0.00325
	313	3.00×10^{-2}	9.58×10^{-5}	–3.51	–9.25	0.00320
	318	3.50×10^{-2}	1.10×10^{-4}	–3.35	–9.12	0.00315
	323	3.90×10^{-2}	1.21×10^{-4}	–3.24	–9.02	0.00310
8	303	1.00×10^{-2}	3.30×10^{-5}	–4.61	–10.32	0.00330
	308	1.10×10^{-2}	3.57×10^{-5}	–4.51	–10.24	0.00325
	313	1.20×10^{-2}	3.83×10^{-5}	–4.42	–10.17	0.00320
	318	1.25×10^{-2}	3.93×10^{-5}	–4.38	–10.14	0.00315
	323	1.30×10^{-2}	4.02×10^{-5}	–4.34	–10.12	0.00310
10	303	2.70×10^{-2}	8.91×10^{-5}	–3.61	–9.33	0.00330
	308	2.80×10^{-2}	9.09×10^{-5}	–3.58	–9.31	0.00325
	313	3.00×10^{-2}	9.58×10^{-5}	–3.51	–9.25	0.00320
	318	3.20×10^{-2}	1.00×10^{-4}	–3.44	–9.20	0.00315
	323	3.40×10^{-2}	1.05×10^{-4}	–3.38	–9.16	0.00310
12	303	2.00×10^{-3}	6.60×10^{-6}	–6.22	–11.93	0.00330
	308	2.50×10^{-3}	8.12×10^{-6}	–5.99	–11.72	0.00325
	313	2.80×10^{-3}	8.95×10^{-6}	–5.88	–11.62	0.00320
	318	3.00×10^{-3}	9.43×10^{-6}	–5.81	–11.57	0.00315
	323	3.40×10^{-3}	1.05×10^{-5}	–5.68	–11.46	0.00310
14	303	1.50×10^{-2}	4.95×10^{-5}	–4.20	–9.91	0.00330
	308	2.20×10^{-2}	7.14×10^{-5}	–3.82	–9.55	0.00325
	313	2.25×10^{-2}	7.99×10^{-5}	–3.79	–9.44	0.00320
	318	2.40×10^{-2}	7.55×10^{-5}	–3.73	–9.49	0.00315
	323	2.90×10^{-2}	9.98×10^{-5}	–3.54	–9.32	0.00310

From Table 1, the values of k_obs increased systematically with rising temperature across all pH levels, highlighting the thermally activated nature of the reaction. Figures a-e illustrate the concentration-time profiles of Mn(VII) reduction at different pH values for each temperature condition. At 303 K (Figure 1), the reduction proceeded more slowly, requiring longer times for significant conversion. In contrast, at 323 K (Figure 5), the process was substantially faster, with near-complete reduction achieved within 120 seconds.

The effect of pH was also pronounced. The rate of Mn(VII) reduction was consistently higher in alkaline media than in acidic or neutral conditions. This behavior is explained by the stability and higher reactivity of the free sulfide ion (S^{2-}) under alkaline conditions, where it exists predominantly in its fully deprotonated form. In contrast, at lower pH, S^{2-} undergoes protonation to form HS^- or H_2S, which reduces the effective concentration of the active reductant [23,24].

In addition, the formation and precipitation of $Mn(OH)_2$ in alkaline solutions help drive the equilibrium toward product formation, further accelerating the observed reduction rate. Overall, the kinetic results confirm a first-order dependence on Mn(VII), with the rate law:

$$\text{Rate} = -\frac{d[MnO_4^-]}{dt} = -\frac{d[S^{2-}]}{dt} = k[MnO_4^-][S^{2-}]$$

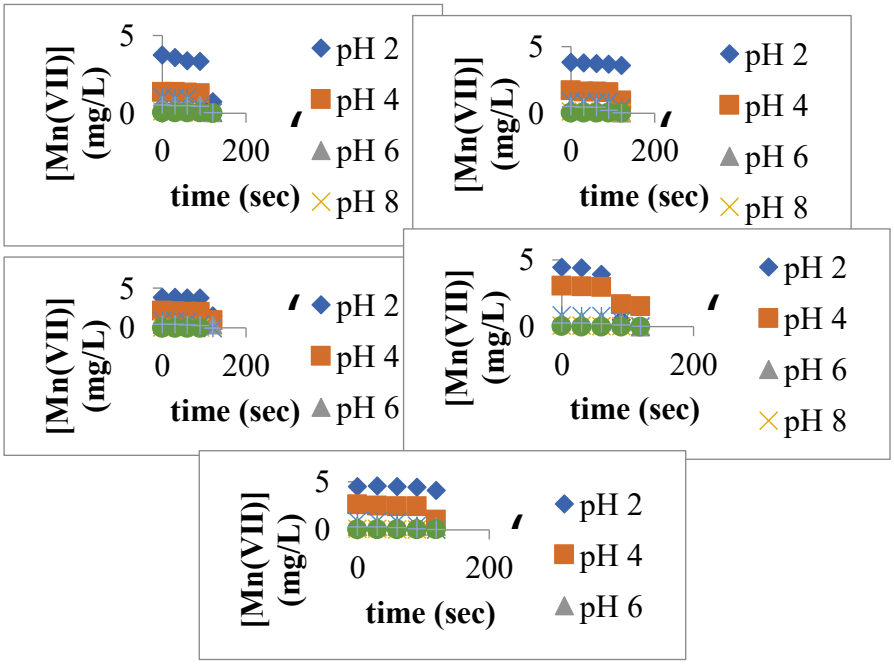

Figure 1. Concentration–time profiles for the reduction of Mn(VII) by sulphide ion at different temperatures and pH conditions: (a) 303 K, (b) 308 K, (c) 313 K, (d) 318 K, and (e) 323 K. Each curve represents a different pH value (2–14), showing that the rate of reduction increases with both rising temperature and alkalinity.

These findings demonstrate that both temperature and pH strongly influence the rate of Mn(VII) reduction by sulphide ion, with the most favorable conditions being alkaline pH and elevated temperatures.

4.2 Thermodynamic Parameters

The thermodynamic parameters derived from the Eyring plots are summarized in Table 2.

Table 2. Activation enthalpy (ΔH°) and entropy (ΔS°) for Mn(VII) reduction by S^{2-} at 25 °C

pH	ΔH° (kJ/mol)	ΔS° ($J \cdot K^{-1} \cdot mol^{-1}$)
2	29.93	1.12
4	43.40	1.15
6	25.28	1.11

7	8.31	1.05
10	7.32	1.05
12	18.13	1.14
14	20.62	1.09

The calculated activation enthalpy (ΔH°) values were negative (–43.40 to –7.32 kJ mol^{-1}), suggesting that the reduction of Mn(VII) by sulphide ion is an exothermic process, releasing heat and therefore thermodynamically favorable [25,26]. The negative ΔH° values imply that the reaction does not require continuous energy input once initiated.

The entropy changes (ΔS°) were positive (1.05–1.15 J K^{-1} mol^{-1}), indicating increased disorder in the system. This reflects a dissociative mechanistic pathway where the transition state leads to the production of additional ions or gas molecules, thereby enhancing system randomness [15].

The activation energies (Ea), summarized in Table 3, were all positive and ranged between 9.91 and 45.96 kJ mol^{-1}.

Table 3. Activation energy (Ea) for Mn(VII) reduction by S^{2-} at different pH

pH	Ea (kJ/mol)
2	35.14
4	45.96
6	27.82
7	10.84
10	9.91
12	20.70
14	23.36

These moderate activation energy values confirm that the Mn(VII)–S^{2-} redox system is kinetically accessible under the studied conditions, with lower Ea values observed under alkaline pH, consistent with enhanced reactivity in basic media.

4.3 Reaction Stoichiometry

The stoichiometric aspects of Mn(VII) reduction by S^{2-} were examined by varying the concentration of sulphide ion while monitoring Mn(VII) consumption. The results are summarized in Table 4.

Table 4. Mn(VII) consumption at varying S^{2-} concentrations

S^{2-} (mg/L)	Consumed Mn(VII) (mg/L)
4	0.924
6	1.385
8	1.847
10	2.309
12	2.771

The data show that increasing S^{2-} concentration resulted in proportionate increases in Mn(VII) consumption. For instance, 4 mg/L of S^{2-} consumed 0.924 mg/L of Mn(VII), corresponding to a Mn(VII):S^{2-} ratio of approximately 0.23:1. This stoichiometric relationship remained consistent across concentrations ranging from 4–12 mg/L at pH 9, suggesting that the Mn(VII):S^{2-} ratio is independent of pH under the experimental conditions [15].

The overall stoichiometric reactions for Mn(VII) reduction are represented as follows:

- In acidic medium:

$$2\mathrm{MnO_4^-} + 5\mathrm{S^{2-}} + 16\mathrm{H^+} \rightarrow 2\mathrm{Mn^{2+}} + 5S + 8H_2O \quad (3)$$

- In alkaline medium:

$$2\mathrm{MnO_4^-} + 3\mathrm{S^{2-}} + 4H_2O \rightarrow 2\mathrm{MnO_2} + 3S + 8OH^- \quad (4)$$

These equations confirm that while Mn(VII) reduction invariably yields lower oxidation states of manganese, the final products differ depending on pH. In acidic medium, soluble Mn(II) ions predominate, whereas in alkaline medium, insoluble MnO_2 precipitates as the major product [20].

4.4 Summary of Findings

The combined kinetic, thermodynamic, and stoichiometric analyses provide a comprehensive understanding of Mn(VII) reduction by sulphide ion. The reaction is:

i Kinetically enhanced at higher temperatures and alkaline pH.
ii Thermodynamically favorable, being exothermic with positive entropy contributions.
iii Stoichiometrically consistent, yielding a Mn(VII):S^{2-} ratio of ~0.23:1 across conditions.

These findings underscore the dual significance of sulphide ion as both a potent reductant and a facilitator of manganese precipitation, making the Mn(VII)/S^{2-} system highly relevant in environmental remediation and wastewater treatment [23–26].

5.0 Conclusion and Recommendations

5.1 Conclusion

This study has demonstrated that sulphide ion (S^{2-}) effectively reduces Mn(VII) in aqueous solution to more stable and less oxidizing lower oxidation states. The reduction process was strongly influenced by both **temperature** and **pH**, with higher temperatures and alkaline conditions significantly accelerating the rate of Mn(VII) consumption. Kinetic analysis confirmed a first-order dependence on Mn(VII), with observed rate constants (k_obs) increasing systematically under alkaline media due to the greater availability and reactivity of S^{2-}. Thermodynamic evaluations revealed negative activation enthalpy (ΔH°) values, confirming the exothermic and spontaneous nature of the process, while positive entropy (ΔS°) values indicated a dissociative mechanistic pathway. The reaction stoichiometry was consistent across varying concentrations of S^{2-}, yielding an Mn(VII): S^{2-} ratio of approximately 0.23:1, independent of pH.

Beyond simple reduction, the study highlights that Mn(VII)/S^{2-} interactions can generate intermediate manganese species (Mn(III), Mn(V), Mn(VI)) and reactive sulphate radicals ($SO_4^{2\bullet-}$), which are known to possess strong oxidative capabilities. These intermediates enhance the system's potential for the degradation of organic and inorganic pollutants, making the Mn(VII)/S^{2-} system highly relevant for water and wastewater treatment applications [23,27–30]. The dual role of sulphide, both as a reductant and as an activator of reactive species, positions it as a versatile agent in environmental remediation strategies.

5.2 Recommendations

i Future studies should explore the selective use of different sulphide species and reaction conditions to optimize Mn(VII) reduction while minimizing the formation of undesirable by-products or the co-reduction of other metals.

ii Integration of sulphide-based Mn(VII) reduction with complementary treatment methods such as adsorption, advanced oxidation processes, or biological systems should be investigated to develop more holistic and efficient remediation approaches.

iii Research into functionalized or modified sulphide materials may provide enhanced reactivity and selectivity, improving the efficiency of Mn(VII) reduction under diverse environmental conditions.

iv The feasibility of using waste-derived sulphide sources should be considered as a **cost-effective and** sustainable alternative**,** aligning with circular economy principles for large-scale environmental applications.

In summary, this work not only clarifies the kinetics, thermodynamics, and stoichiometry of Mn(VII) reduction by S^{2-} but also provides a scientific basis for advancing sulphide-based technologies in environmental and industrial systems.

Declarations

Funding
This research received no specific grant from any funding agency in the public, commercial, or not-for-profit sectors.

Conflicts of Interest
The authors declare that there are no conflicts of interest regarding the publication of this paper.

Availability of Data and Materials
All data generated or analyzed during this study are included in this manuscript. Additional datasets, if required, are available from the corresponding author upon reasonable request.

Authors' Contributions
Targema Rosemary D: Conceptualization, Methodology, Experimental design, Data collection, Writing original draft.
Tivkaa Joseph T: Data analysis, Validation, Writing review, and Editing.
Atagher: Supervision, Critical review of the manuscript, Project administration.
All authors have read and approved the final version of the manuscript.

Ethical Approval
This study did not involve human participants or animals; hence, ethical approval was not required.

Consent to Participate
Not applicable.

Consent for Publication
All authors consent to the publication of the manuscript in Frontiers and Results in Applied Sciences.

References

[1] S. R. Taylor and S. M. McLennan, "The Geochemical Evolution of Continental Crust," *Rev. Geophys.*, vol. 33, no. 2, pp. 241–265, 1995.

[2] W. Li, X. H. Chen, L. S. Xie, X. Liu, and X. Y. Xiong, "Bioelectrochemical systems for groundwater remediation: The development trend and research front revealed by bibliometric analysis," *Water*, vol. 11, no. 8, p. 1532, 2019.

[3] R. K. Gautam, S. Soni, and M. C. Chattopadhyaya, "Functionalized magnetic nanoparticles for environmental remediation," in *Handbook of Research on Diverse Applications of Nanotechnology in Biomedicine, Chemistry and Engineering*, Ideal Group, U.S.A, 2014, pp. 518–551.

[4] M. Oves, K. M. Saghir, Q. A. Huda, F. M. Nadeen, and T. Almeelbi, "Heavy metals: Biological importance and detoxification strategies," *J. Bioremed. Biodeg.*, vol. 7, no. 2, pp. 1–15, 2016.

[5] S. Sidiquee, K. Rovina, and S. A. Azad, "Heavy metal contaminants removal from wastewater using the potential filamentous fungi biomass: A review," *J. Microbiol. Biochem. Technol.*, vol. 7, no. 6, pp. 384–393, 2015.

[6] R. Mehrandish, A. Rahimian, and A. Shahriary, "Heavy metals detoxification: A review of herbal compounds for chelation therapy in heavy metals toxicity," *J. Herbmed. Pharmacol.*, vol. 8, no. 2, pp. 69–77, 2019.

[7] L. Hu, H. M. Martin, and T. J. Strathmann, "Oxidation kinetics of antibiotics during water treatment with potassium permanganate," *Environ. Sci. Technol.*, vol. 44, pp. 6416–6422, 2010.

[8] L. Hu, A. M. Stemig, K. H. Wammaer, and T. J. Strathmann, "Oxidation of antibiotics during water treatment with potassium permanganate: Reaction pathways and deactivation," *Environ. Sci. Technol.*, vol. 45, pp. 3635–3642, 2011.

[9] N. Singh and D. G. Lee, "Permanganate: A green and versatile industrial oxidant," *Org. Process Res. Dev.*, vol. 5, no. 6, pp. 599–603, 2001.

[10] R. H. Waldemer and P. G. Tratnyek, "Kinetics of contaminant degradation by permanganate," *Environ. Sci. Technol.*, vol. 40, no. 3, pp. 1055–1061, 2006.

[11] C. Guan, Q. Guo, Z. Wang, X. Wei, B. Han, X. Luo, H. Pan, and J. Jiang, "Bisulphite activated permanganate for oxidative water decontamination," *Water Res.*, vol. 216, p. 118323, 2022.

[12] H. B. Rollin, "Manganese: Environmental pollution and health effect," in *Encyclopedia of Environmental Health*, J. O. Nriagu, Ed. Burlington: Elsevier, 2011, vol. 3, pp. 617–629.

[13] A. Jayaraman and A. East, "Permanganate oxidation of sulphides and sulphoxides," *J. Org. Chem.*, vol. 77, no. 1, pp. 351–356, 2001.

[14] K. Xu and U. Von Gunten, "Permanganate reduction by hydrogen peroxide: Formation of reactive manganese species and superoxide and enhanced micropollutant abatement," *ACS ES&T Eng.*, vol. 1, no. 10, pp. 1410–1419, 2021.

[15] M. Bouchard, D. Mergler, M. Baldwin, M. Panisset, R. Bowler, and H. A. Roels, "Neurobehavioral functioning after cessation of manganese exposure: A follow-up after 14 years," *Am. J. Ind. Med.*, vol. 50, no. 11, pp. 831–840, 2007.

[16] C. Guan, C. Guan, Q. Guo, R. Huang, J. Duan, Z. Wang, X. Wei, and J. Jiang, "Enhanced oxidation of organic contaminants by Mn(VII) in water," *Water Res.*, vol. 226, p. 119265, 2022.

[17] S. Alonso-Azcarate, S. H. Bottrell, and J. Trilla, "Sulphur redox reactions and formation of native sulphur veins during low-grade metamorphism of gypsum evaporites, Cameros Basin (NE Spain)," *Chem. Geol.*, vol. 174, no. 4, pp. 389–402, 2001.

[18] O. Kabil and R. Banerjee, "Redox biochemistry of hydrogen sulphide," *J. Biol. Chem.*, vol. 285, no. 29, pp. 21903–21907, 2010.

[19] Y. Lu, Q. He, and H. A. Gasteiger, "Probing the lithium–sulphur redox reactions: A rotating ring disk electrode study," *J. Phys. Chem. C*, vol. 118, no. 11, pp. 5733–5741, 2014.

[20] M. S. Iorungwa, R. A. Wuana, S. G. Yiase, and T. A. Tor-Anyiin, "A kinetic, thermodynamic and stoichiometric study on the reductive detoxification of Cr(VI) in aqueous phase by sodium metabisulphite," *J. Environ. Earth Sci.*, vol. 16, no. 4, pp. 61–71, 2014.

[21] J. G. O. Marques, A. L. Casta, and C. Pereira, "Gibbs free energy (ΔG) analysis for the Na–O–H thermochemical water splitting cycle," *Int. J. Hydrogen Energy*, vol. 44, no. 29, pp. 14536–14549, 2019.

[22] S. A. Ashter, *Thermoforming of Single and Multilayer Laminates: Plastic Films Technologies, Testing and Application*, pp. 133–145.

[23] H. A. Firouzjaile and W. E. Mustain, "Catalytic advantages, challenges and priorities in alkaline membrane fuel cells," *ACS Appl. Energy Mater.*, vol. 10, no. 1, pp. 225–234, 2020.

[24] A. Najah, F. Asjaoli, and A. A. Safari, "Effect of sulphide and hydroxide on the removal of heavy metal ions from hydrometallurgical zinc effluent," *Int. J. Environ. Anal. Chem.*, vol. 104, no. 18, pp. 1–15, 2022.

[25] S. Ghobadi, B. Samiey, and A. Ghanbari, "Adsorption and reduction coupling of permanganate on MoS_2: Water treatment and metal ion separation," *J. Solid State Chem.*, vol. 304, p. 122588, 2021.

[26] D. Rao, J. Chen, H. Dong, J. Qiao, B. Zhou, Y. Sun, and X. Guan, "Enhanced oxidation of organic contaminants by Mn(VII)/$CaSO_3$ under environmentally relevant conditions: Performance and mechanisms," *Water Res.*, vol. 188, p. 116481, 2021.

[27] L. Feng, H. Yin, T. Zhu, and W. Zhuang, "Understanding the role of manganese oxides in retaining harmful metals: Insights into oxidation and adsorption mechanisms at microstructure level," *Eco-Environment Health*, vol. 3, no. 1, pp. 89–106, 2024.

[28] D. Luo, H. Zhang, X. An, J. Zhao, C. Feng, J. Yin, M. Luo, T. Wei, Y. Liu, Y. Shi, J. Zhang, and B. Lai, "Synergistic effects of sulphur-doped carbon dots/permanganate process for DCF degradation: Mechanism and pathways," *J. Hazard. Mater.*, vol. 495, p. 138567, 2025.

[29] H. Zhang and F. W. Schwartz, "Simulating the in situ oxidation treatment of chlorinated ethylenes by potassium permanganate," *Water Resour. Res.*, vol. 36, no. 10, pp. 3031–3042, 2000.

[30] L. Hu, H. M. Martin, O. Arce-Bulted, M. N. Sugihara, K. A. Keeting, and T. J. Strathmann, "Oxidation of carbamazepine by Mn(VII) and Fe(VI): Reaction kinetics and mechanism," *Environ. Sci. Technol.*, vol. 43, no. 2, pp. 509–515, 2009.